

Journal Pre-proofs

Anion-directed Assembly of Three Cationic Silver(I) Coordination Polymers with Bis(imidazolyl)-based Linker: Structural Characterization and Anion Exchange Study

Sara Azizzadeh, Valiollah Nobakht, Lucia Carlucci, Davide M. Proserpio

PII: S0277-5387(19)30681-3
DOI: <https://doi.org/10.1016/j.poly.2019.114236>
Reference: POLY 114236

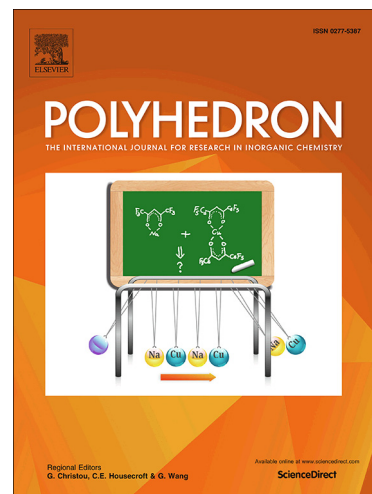
To appear in: *Polyhedron*

Received Date: 10 June 2019
Revised Date: 23 September 2019
Accepted Date: 3 November 2019

Please cite this article as: S. Azizzadeh, V. Nobakht, L. Carlucci, D.M. Proserpio, Anion-directed Assembly of Three Cationic Silver(I) Coordination Polymers with Bis(imidazolyl)-based Linker: Structural Characterization and Anion Exchange Study, *Polyhedron* (2019), doi: <https://doi.org/10.1016/j.poly.2019.114236>

This is a PDF file of an article that has undergone enhancements after acceptance, such as the addition of a cover page and metadata, and formatting for readability, but it is not yet the definitive version of record. This version will undergo additional copyediting, typesetting and review before it is published in its final form, but we are providing this version to give early visibility of the article. Please note that, during the production process, errors may be discovered which could affect the content, and all legal disclaimers that apply to the journal pertain.

© 2019 Elsevier Ltd. All rights reserved.



Anion-directed Assembly of Three Cationic Silver(I) Coordination Polymers with Bis(imidazolyl)-based Linker: Structural Characterization and Anion Exchange Study

Sara Azizzadeh,^[a] Valiollah Nobakht,^{*[a]} Lucia Carlucci,^[b] Davide M. Proserpio^{[b],[c]}

[a] Department of Chemistry, Faculty of Sciences, Shahid Chamran University of Ahvaz, Ahvaz, Iran. Fax: +98 613 3331042; E-mail: v.nobakht@scu.ac.ir

[b] Dipartimento di Chimica, Università degli Studi di Milano, Via C. Golgi 19, 20133, Milano, Italy.

[c] Samara Center for Theoretical Materials Science (SCTMS) Samara State Technical University, Samara 443011, Russia.

Abstract

Three cationic silver(I) coordination polymers, namely $\{[\text{Ag}_2(\mu\text{-bib})_3](\text{SO}_3\text{CF}_3)_2 \cdot (\text{CH}_3\text{CN})\}_n$ (**1**), $\{[\text{Ag}(\mu\text{-bib})](\text{NO}_3) \cdot (\text{H}_2\text{O})\}_n$ (**2**), and $\{[\text{Ag}(\mu\text{-bib})]\text{BF}_4\}_n$ (**3**), have been prepared using flexible bis(imidazolyl)butane (bib) ligand and silver salts of different anions. All compounds are characterized by FT-IR, PXRD, elemental analysis, and single-crystal X-ray diffraction. Compound **1**, containing triflate (SO_3CF_3^-) anion, exhibits a two dimensional **6³-hcb** network with an amazing ABCDEF packing mode of the single hexagonal layers. Compound **2**, containing nitrate ions, forms a simple one dimensional wavy chain, while compound **3** with BF_4^- anions, shows a double helix DNA-shaped structure stabilized by $\text{Ag} \cdots \text{Ag}$ interactions between the two strands. The anions in the structures **1-3** are non-coordinating and participate in weak H-bonding, while imidazolyl rings are involved in $\pi \cdots \pi$ stacking interactions. Anion exchange experiments in aqueous solution, monitored by FT-IR and PXRD analyses, reveal interesting structural transformations.

Keywords: Coordination polymer, silver(I), anion exchange, structural transformation, anion effect.

Introduction

Research towards self-assembled coordination polymers (CPs), containing metal ions and multitopic organic linkers, has rapidly grown over the past three decades. This is because of the fascinating structural features of CPs, their versatile properties, and wide range of potential applications in heterogeneous catalysis, gas separation and storage, biomedicine, optics, electronic devices and so on.^[1] Among various metal ions, used in the synthesis of CPs, silver(I) with d^{10} electronic configuration is particularly interesting, not only because of its adaptable coordination geometry which can generate diverse networks, but also for its photoluminescence and antibacterial properties.^[2] It is quite well known that in the self-assembly process rigid ligands are required for purposeful design of predictable networks, and usually, such type of ligands are involved in the construction of metal organic frameworks (MOFs); on the other hand, flexible ligands often lead to greater structural diversity and less predictable architectures.^[3] Even so, CPs containing flexible ligands show interesting host-guest features, structural transformation and more sensitivity towards external stimuli.^[4] Flexible networks can reversibly change to fit the guest molecules, and this flexibility can also greatly enhance the mechanical properties of nets.^[5, 1a] The topology of frameworks containing silver(I) ion and flexible linkers is affected by several factors including the reaction condition, metal-to-ligand ratio, ligand geometry, coordination potential of the anions, as well as, non-covalent H-bonding, $\pi \cdots \pi$, C-H $\cdots\pi$ and Ag \cdots Ag interactions.^[6] Hence, silver(I) ion coordinated to a bidentate linker can form various 1D to 3D architectures. In this regard and, as a continuation of our previous work on the synthesis of CPs based on flexible ligands^[7], here we report on the reactivity of a flexible bis(imidazolyl) butane ligand with silver(I) salts of three different counter-anions, SO_3CF_3^- , NO_3^- , and BF_4^- . In the presence of these weakly- or non-coordinating anions, silver centers can show their intrinsic nature to select a favorite coordination geometry. The result is the

isolation of a 2D honeycomb (**6³-hcb**) net with fascinating crystal packing and two 1D compounds showing chain or helical DNA-shaped structures. In addition, anion exchange behavior and structural transformation of the compounds have been investigated.

Experimental

Materials and Physical Measurements

All experiments are carried out in air. The starting materials are purchased from commercial sources and used without further purification. The bib linker is prepared according to the published method.^[8] Infrared spectra (4000–400 cm⁻¹) are recorded from KBr disks with a BOMEN MB102 FT-IR spectrometer. Elemental analyses for C, H and N are performed on a CHNSO Elementar Vario EL III apparatus. X-ray powder diffraction patterns are recorded on a Philips X'Pert Pro diffractometer (Cu K α radiation, $\lambda = 1.54184 \text{ \AA}$) in the 5–45° 2 θ range. The simulated PXRD patterns based on the single crystal X-ray diffraction data are prepared using Mercury software.^[9]

Synthetic Procedures

Preparation of $\{[\text{Ag}_2(\mu\text{-bib})_3](\text{SO}_3\text{CF}_3)_2 \cdot (\text{CH}_3\text{CN})\}_n$ (**1**)

A solution of bib (0.044 g, 0.23 mmol) in CH₃CN (4 mL) is gently layered on the top of an aqueous solution (4 mL) of AgSO₃CF₃ (0.03 g, 0.12 mmol) in a test tube and kept in a dark place. Colorless crystals of **1**, suitable for X-ray diffraction, are obtained after two weeks. The crystals are collected and dried in air (0.05 g, 71% based on Ag). Anal. Calcd for C₃₄H₄₅Ag₂N₁₃F₆O₆S₂: C 36.28, H 4.03, N 16.18; Found: C 36.43, H 3.86, N 16.06%.

Preparation of $\{[\text{Ag}(\mu\text{-bib})](\text{NO}_3) \cdot (\text{H}_2\text{O})\}_n$ (**2**)

bib (0.25 g, 1.31 mmol) is added to a solution of AgNO₃ (0.15 g, 0.88 mmol) in DMSO (15 mL). The resulting reaction mixture is stirred for 12 h at room temperature and then filtered.

Colorless cubic single crystals of **2**, suitable for X-ray diffraction, are obtained at room temperature by slow evaporation of the solvent after two weeks. They are collected, washed with EtOH and dried in air (0.28 g, 70% yield based on Ag). Anal. Calcd for $C_{10}H_{16}AgN_5O_4$: C 31.76, H 4.26, N 18.52; Found: C 31.67, H 3.80, N 18.56%.

Preparation of $\{[Ag(\mu\text{-bib})]BF_4\}_n$ (**3**)

A solution of bib (0.044 g, 0.23 mmol) in CH_3CN (4 mL) is gently layered on the top of an aqueous solution (4 mL) of $AgNO_3$ (0.02 g, 0.12 mmol) and $NaBF_4$ (0.015 g, 0.14 mmol) in a test tube and kept in a dark place. Colorless crystals of **3**, suitable for X-ray diffraction, are obtained after a week. The crystals are collected and dried in air (0.03 g, 50% based on Ag). Anal. Calcd for $C_{10}H_{16}AgN_5O_4$: C 31.20, H 3.67, N 14.56; Found: C 31.04, H 3.48, N 14.71%.

Anion Exchange in Solution

A well-powdered sample of **1'** (new crystalline phase **1** at r.t.) (0.05 g, 0.09 mmol) is suspended in 10 mL of water containing 0.09 mmol of, respectively, KNO_3 , $NaBF_4$ and $NaClO_4$ salts. The mixtures are stirred at room temperature for 1 day. The resulting anion-exchanged solids are separated by centrifugation, washed several times with water, EtOH and Et_2O and dried in air to give exchanged products **1'**- NO_3 , **1'**- BF_4 , and **1'**- ClO_4 . Similarly, anion exchange behaviour of compound **2** has been explored in solutions of KSO_3CF_3 , $NaBF_4$, and $NaClO_4$ to give anion exchanged products **2**- SO_3CF_3 , **2**- BF_4 , and **2**- ClO_4 . To investigate the reversibility of anion exchange between compounds **1'** and **2**, the compounds **2** or **1'** were immersed in an equimolar solution of KSO_3CF_3 or KNO_3 , respectively.

Single Crystal X-ray Crystallographic Studies

X-ray data are collected on a Bruker Apex II diffractometer using MoK α radiation. The structures are solved using direct methods and refined using a full-matrix least squares procedure based on F^2 using all data.^[10] Hydrogen atoms are placed at geometrically estimated positions. Details relating to the crystals and the structural refinements are presented in Table 1. Full details of crystal data and structure refinements, in CIF format, are available as Supporting Information. CCDC reference numbers 1867058-1867060 for **1-3**.

Results and discussion

Synthesis of compounds **1-3**.

To investigate the effect of counter anion on the structure of Ag(I) CPs, the reaction of bidentate bib ligand with different silver(I) salts in a molar ratio of 2:1 has been investigated at room temperature. The result is the isolation and characterization of three new cationic one- or two-dimensional polymeric complexes which show interesting structural features (compounds **1** and **3**) and one-dimensional wavy chain structure (compound **2**). The new complexes, that are almost stable towards air and moisture, have been characterized by elemental analyses, FT-IR spectroscopy, PXRD and single-crystal X-ray diffraction.

Crystal structures

Crystal Structure of $\{[Ag_2(\mu\text{-bib})_3](SO_3CF_3)_2 \cdot (CH_3CN)}\}_n$ (**1**)

Compound **1** crystallizes in the monoclinic space group $P2_1/c$ with $Z = 4$ (Table 1). The asymmetric unit consists of two silver(I) ions, three crystallographically independent μ -bib ligands, two $SO_3CF_3^-$ ions and a CH_3CN guest molecule (Figure 1a). Each Ag atom is coordinated by three bib nitrogen atoms to form a slightly distorted trigonal planar AgN_3 environment. The bib ligands bridge the Ag(I) centers to form two-dimensional **hcb** layers with hexagon-shaped $[Ag_6(\text{bib})_6]^{6+}$ metallocycles, as shown in Figure 1b. The flexible nature of the alkyl $-(CH_2)_4-$ linker in the μ -bib ligand provides considerable conformational

freedom. Although the three independent bib ligands in the unit cell have the same *anti-anti-anti* (*aaa*) conformation, their torsion angles and dihedral angle between the two imidazolyl rings belonging to the same bib molecule are slightly different and therefore show three different (Ag)N \cdots N(Ag) distances of 10.333, 10.395 and 10.435 Å. The silver \cdots silver separations in the [Ag₆(bib)₆]⁶⁺ hexagons are, however, almost the same, ranging from 14.216 to 14.279 Å.

The two dimensional layers, shown in different colors in Figure 1c, stack in an uncommon ABCDEFABCDEF... long sequence. Layers A (red) and B (green) stack in such a way that the vertices of hexagons (silver atoms or 3-c nodes) of layer B are located at the centers of the layer A hexagons. Packing of A and B honeycomb layers in **1** is the same as the ABAB packing mode of the layers in the structure of Cu-BTPP [H₃BTPP= 1,3,5- tris((1H-pyrazol-4-yl)phenyl)benzene].^[11] Vertices of hexagons belonging to layers C (orange), E (yellow) and F (violet) occupy the centers of the layer A hexagons but in different ways. Although, the vertices of the D (blue) layer locate at the same places as the layer A, the Ag(imidazolyl)₃ moieties of the layer D are rotated by 60°. A movie of the packing sequence of the sheets is shown in the Supporting Information. Each silver(I) ion show Ag \cdots Ag distances of 3.26 and 3.44 Å with neighboring silver atoms of the adjacent sheets. If these weak interactions are taken into account, the silver became 5-coordinated and the underlying 3D net is the rare 5-c **fnu**. The SO₃CF₃⁻ anions accommodate between the 2D layers with no significant interactions with the Ag(I) centers. However, the SO₃CF₃⁻ anions show non-classic C-H \cdots O interactions^[12] with hydrogen atoms of the bib linkers as shown in Figure 2. Half of these interactions connect adjacent sheets and form a 3D supramolecular architecture. The guest CH₃CN molecule also interacts with a hydrogen atom of an imidazolyl ring. Details of the hydrogen bonding geometry are reported in Table 2.

$\pi \cdots \pi$ stacking interactions between the imidazolyl rings of the ligands are also recognized.^[13] The results are shown graphically in Figure 3. These $\pi \cdots \pi$ stacking interactions between layers A and C, B and D, C and E, and D and F, stabilize the structure in the 3D crystal packing. The total void value of the channels without guest molecules is estimated (by Platon)^[14] to be 522.8 Å³, approximately 11.4% of the unit cell volume. Just recently, two-dimensional metal-organic framework (known as 2D MOFs) monolayers or nano-sheets have emerged as a new member of 2D materials with promising properties and applications.^[15] In this regard, compound **1** with weak intra-layer interactions of types $\pi \cdots \pi$ stacking and long range Ag \cdots Ag may be easily exfoliated to its 2D monolayers with highly ordered pore arrays in plane and highly accessible active sites on the large surface.

Crystal Structure of {[Ag(μ -bib)](NO₃)·(H₂O)}_n (**2**)

Compound **2** crystallizes in the orthorhombic space group $P2_12_12_1$ with $Z = 4$. The structure consists of parallel polymeric wavy chains as indicated in Figure 4. All chains within the crystal are parallel and extend along the c axis. The Ag(I) centers are bound to two imidazolyl rings from separate ligands with N-Ag-N angle close to linearity [172.30(8)°].

A water molecule also traps in the unit cell and show weak interaction with silver ion. The Ag \cdots O distance [2.803(3) Å] is somewhat longer than a typical interaction between Ag(I) and an aqua ligand (2.622 Å).^[16] The nitrate anions are located on alternate sides of the zig-zag [Ag(μ -bib)]_n⁺ chain and interact through hydrogen bonding with water guest molecules, H \cdots O distances of 2.00(4) Å and 2.03(4) (Table 2). These hydrogen bonds form 1D zig-zag chains running along the a axis and perpendicular to the direction of the [Ag(μ -bib)]_n⁺ chains (Figure 5). In addition, weaker non-classic C-H \cdots O interactions^[12] are also observed between O atoms of the nitrate ions or water molecules and CH groups of μ -bib ligands (Table 2).

The μ -bib ligands exhibit *gauche-gauche-anti* (*gga*) conformation for the $-(\text{CH}_2)_4-$ spacer with $(\text{Ag})\text{N}\cdots\text{N}(\text{Ag})$ distance of 7.230 Å and $\text{Ag}\cdots\text{Ag}$ separation of 8.115 Å. The ligand length in **2** is remarkably (ca. 3.1 Å) shorter than that observed in **1** (10.33-10.44 Å) for ligands with extended *aaa* conformation, however, is comparable with those reported for the *gag* μ -bib ligands in the structure of $\{[\text{Zn}(\mu\text{-bib})_2](\text{ClO}_4)_2\cdot(\text{Et}_2\text{O})_{0.5}\cdot(\text{H}_2\text{O})_{0.25}\}_n$ ^[17] and $\{[\text{Co}(\text{bib})_3](\text{PF}_6)_2\}_n$ ^[18]. The *gaa*, *gag*, and *gga* conformations usually provide shorter ligand length and subsequently shorter metal \cdots metal separation with respect to the *anti-anti-anti* one.^[7a] Significant $\pi\cdots\pi$ stacking interactions occur in **2** between two adjacent chains, that are characterized by imidazole centroid \cdots centroid distance and dihedral angle of 3.6692(14) Å and 4.45(14)°, respectively^[13] (Figure S1).

Crystal Structure of $\{[\text{Ag}(\mu\text{-bib})](\text{BF}_4)\}_n$ (**3**)

Compound **3** crystallizes in the monoclinic space group $C2/c$ with $Z = 8$. The asymmetric unit consists of two Ag(I) ions which lie on twofold crystallographic axis, one bib ligand and one BF_4^- anion (Figure 6). The crystallographically independent Ag(I) ions are coordinated by the bib ligands with almost linear N-Ag-N angles of 178.70(11) and 179.89(10)° to form 1D helical coordination polymer, running along the a axis. The Ag–N distances of 2.099(2) and 2.092(3) Å are consistent with that found in compounds **1** and **2** and also in other reported Ag(I) complexes of N-donor ligands. Interestingly, pairs of one dimensional helical chains are held together by $\text{Ag}\cdots\text{Ag}$ interactions of 2.9856(6) Å to form double helix DNA-shaped structure.^[19] The $\text{Ag}\cdots\text{Ag}$ distance is slightly longer than the Ag–Ag separation in metallic silver (2.89 Å) but shorter than the sum of the van der Waals radii of silver atoms (3.44 Å).^[20] As a result of the $\text{Ag}\cdots\text{Ag}$ interactions, tetranuclear 24-membered $[\text{Ag}_4(\text{bib})_2]^{4+}$ metallocycles form along the double helix chains with each silver(I) ion adopting a T-shaped

geometry. These interactions stabilize the double strand helix, showing a similar role as the weak interactions between the two helical chains of a DNA in biological systems.

The coordinated μ -bib ligands show *gauche-anti-anti* (*gaa*) conformation with (Ag)N \cdots N(Ag) distance of 8.698 Å and Ag \cdots Ag separation of 11.452 Å. So, the ligand length is shorter than those observed in **1**, where the ligands have *aaa* conformation, but longer than the one observed in **2** with *gga* conformation. The dihedral angle between the mean planes of the imidazolyl rings of the bib ligand is 3.8(2)°.

BF₄⁻ ions are accommodated between the double strand chains and show non-classic C-H \cdots F interactions between F atoms and CH groups of μ -bib ligands (Table 2, Figure S2).^[12] As shown in Figure S2, each BF₄⁻ ions connect three neighboring chains and form a single 3D hydrogen bonded supramolecular architecture. $\pi\cdots\pi$ stacking interactions are also observed between the imidazolyl rings of adjacent chains which show centroid \cdots centroid distance of 3.776(2) Å and dihedral angle of 3.8(2)°.^[13]

Spectroscopic Characterization

Infrared spectra of **1'-3** exhibit characteristic bands of the coordinated bib ligands and also typical absorption bands for the SO₃CF₃⁻, NO₃⁻, and BF₄⁻ anions (Figure S3). The peaks observed at 2850-2960 cm⁻¹ are assigned to the symmetric and asymmetric stretching vibrations of the methylene (-CH₂)_n groups of the butyl spacer of the ligands and the other peaks at about 3125 cm⁻¹ are attributed to the stretching vibrations of sp² C-H bonds of the imidazolyl rings. The spectrum of **1'** exhibits several bands with medium to strong intensity corresponding to the presence of triflate ions. The strong bands at 1255 and 1277 cm⁻¹ are attributed to the asymmetric $\nu_{as}(\text{SO}_3)$ stretching modes while the band with medium intensity at 1028 cm⁻¹ is assigned to the symmetric $\nu_s(\text{SO}_3)$ stretching of the triflate ions. The asymmetric $\nu_{as}(\text{CF}_3)$ and symmetric $\nu_s(\text{CF}_3)$ stretching bands appear at 1224 and 1155 cm⁻¹,

respectively.^[7b, 21] The results confirm non-coordinating character of triflate ions in the structure of **1**. The bands at 1382 and 829 cm^{-1} in the infrared spectrum of **2** are assigned to the stretching vibrational modes of uncoordinated NO_3^- anions.^[2a, 22] In addition, the weak bands in the region 3300 – 3500 cm^{-1} confirm the presence of guest H-bonded water molecules. In the IR spectrum of **3**, the strong broad band in the region 1000–1100 cm^{-1} along with a medium-intensity absorption band at 520 cm^{-1} indicate the presence of BF_4^- ion.^[23] The FT-IR spectra of **1'-3** are consistent with their crystal structures.

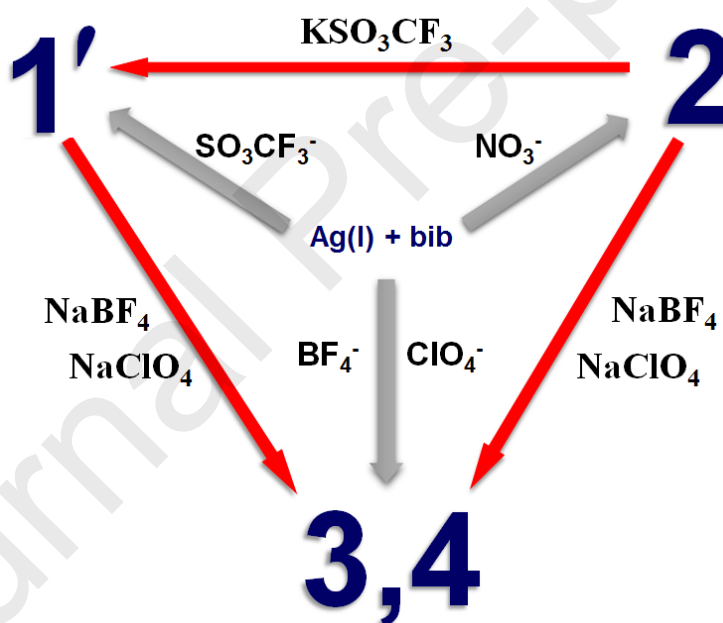
Powder X-ray diffraction (PXRD) experiments were carried out for compounds **1-3** (Figure 7) to confirm the phase purity of the bulk materials. The experimental PXRD patterns show high crystallinity and, except for compound **1**, are consistent with that simulated from the corresponding single crystal X-ray diffraction data. Crystal structure of compound **1** has been determined at low temperature (150 K) and a room temperature structural transformation to a new phase (**1'**), involving the complex stacking of the layers (*vide supra*), maybe the reason for the difference between experimental and calculated PXRD patterns.

Anion Exchange Studies

As revealed by crystal structure analyses, SO_3CF_3^- , NO_3^- , and BF_4^- anions are loosely bound, through weak non-classic hydrogen bonds to the cationic structures of **1'-3**, respectively. Hence, anion exchange properties of the reported compounds have been investigated in aqueous solutions of the appropriate salts and monitored by FT-IR spectroscopy and PXRD analyses.

The disappearance of the triflate peaks in the infrared spectra of the ion-exchanged products of **1'**, (defined as **1'-NO₃**, **1'-BF₄**, and **1'-ClO₄**) and the appearance of new peaks corresponding to the vibration frequencies of NO_3^- , BF_4^- , and ClO_4^- , support the successful exchange of triflates by these anions (Figure 8).

To investigate structural transformations *via* anion exchange process, PXRD patterns of the **1'**-NO₃, **1'**-BF₄, and **1'**-ClO₄ samples have been recorded (Figure 9). Comparison between experimental PXRD patterns of anion exchanged products **1'**-BF₄ and **1'**-ClO₄ with that calculated from single crystal X-ray data of compounds **3** and the isostructural (and isomorphous) {[Ag(μ-bib)]ClO₄}_n **4** (GIMLOE)^[19b] respectively, reveals the transformations of **1'** to the double-helix structures of {[Ag(μ-bib)]X}_n (X= BF₄ and ClO₄), to summarize **1'**-BF₄ = **3** and **1'**-ClO₄ = **4**. Although, FT-IR spectroscopy confirms that the SO₃CF₃⁻ anions in **1** are exchanged by NO₃⁻ ions (Figure 9), the observed PXRD pattern of **1'**-NO₃ doesn't correspond to the calculated pattern of compound **2**, suggesting the formation of a new crystalline phase of possible formula {[Ag(μ-bib)](NO₃)₂}_n.



Scheme I. Details of anion exchange experiments on CPs **1'**-**4**.

Ion exchange experiments on compound **2** are monitored by FT-IR spectroscopy and PXRD analysis (Figure S4 and Figure 10). The results reveal the replacement of the nitrate ions by SO₃CF₃⁻, BF₄⁻, and ClO₄⁻ to give, respectively, **1'**, **3** and **4**, suggesting, also, the reversible exchange between triflate and nitrate ions (Scheme I). Further anion exchange experiments

on **2**-BF₄ (or **3**) and **2**-ClO₄ in KNO₃ solution show no exchange of both BF₄⁻ and ClO₄⁻ by nitrate ion, suggesting, in this case, an irreversible exchange process between NO₃⁻ and BF₄⁻ or ClO₄⁻. This latter observation is also supported by the fact that compound **3** is synthesized by reacting the bib ligand with silver nitrate in the presence of a slight excess of NaBF₄. Anion exchange experiments on **1'** in the presence of a mixture of NO₃⁻ and BF₄⁻ anions resulted formation of **1'**-BF₄ (= **3**) as a single product. The observation can suggest a possibility that the compound with BF₄⁻ could be more stable than that of with NO₃⁻ anion.

Conclusions

Three new cationic Ag(I) CPs of a flexible ligand and weakly coordinating anions, SO₃CF₃⁻, BF₄⁻, and NO₃⁻, have been successfully isolated *via* simple crystallization methods. The results show that the nature and shape of the anions, their interactions with the cationic [Ag(μ-bib)_x]ⁿ⁺ (x = 1 or 1.5) skeleton together with the argentophilic and π···π stacking interactions are the most important factors orienting the stereochemistry of these coordination architectures. Successful anion exchange experiments show the relationship between the reported structures and in particular that spherical anions (BF₄⁻ and ClO₄⁻) favour the double helix motif.

Acknowledgements

The authors thank Shahid Chamran University of Ahvaz (Grant No.: SCU.SC98.206) and the Università degli Studi di Milano (UNIMI) for financial support. DMP acknowledges UNIMI for the transition grant PSR2015-1718.

References

- [1] (a) W. L. Leong, J. J. Vittal, *Chem. Rev.* **2011**, 111, 688-764.; (b) F. Novio, J. Simmchen, N. Vázquez-Mera, L. Amorín-Ferré, D. Ruiz-Molina, *Coord. Chem. Rev.* **2013**, 257, 2839-2847; (c) E. Yashima, N. Ousaka, D. Taura, K. Shimomura, T. Ikai, K. Maeda, *Chem. Rev.* **2016**,

- 116, 13752–13990; (d) D. Tanaka, A. Henke, K. Albrecht, M. Moeller, K. Nakagawa, S. Kitagawa, J. Groll, *Nat. Chem.* **2010**, 410–416.
- [2] (a) A. Tabacaru, C. Pettinari, F. Marchetti, C. di-Nicola, K. V. Domasevitch, S. Galli, N. Masciocchi, S. Scuri, I. Grappasonni, M. Cocchioni, *Inorg. Chem.* **2012**, 51, 9775–9788.; (b) A. Beheshti, S. S. Babadi, P. Mayer, C. T. Abrahams, H. Motamedi, D. Trzybiński, K. Wozniak, *Cryst. Growth Des.* **2017**, 17, 5249–5262.; (c) A. Beheshti, K. Nozarian, S. S. Babadi, S. Noorzadeh, H. Motamedi, P. Mayer, G. Bruno, H. A. Rudbari, *J. Solid State Chem.* **2017**, 249, 70–79.
- [3] L. Carlucci, G. Ciani, D. M. Proserpio, T.G. Mitina, V.A. Blatov, *Chem. Rev.* **2014**, 114, 7557.
- [4] (a) D. Bradshaw, J. E. Warren, M. J. Rosseinsky, *Science*, **2007**, 315, 977–980; (b) J. J. Vittal, *Coord. Chem. Rev.* **2007**, 251, 1781.; (c) M. P. Suh, Y. E. Cheon, E. Y. Lee, *Chem. –Eur. J.* **2007**, 13, 4208–4215; (d) W. Kaneko, M. Ohba, S. Kitagawa, *J. Am. Chem. Soc.* **2007**, 129, 13706–13712.; (e) Z.-Y. Du, T.-T. Xu, B. Huang, Y.-J. Su, W. Xue, C.-T. He, W.-X. Zhang, X.-M. Chen, *Angew. Chem. Int. Ed.* **2015**, 54, 914–918.
- [5] (a) Z.-X. Zhang, N.-N. Ding, W.-H. Zhang, J.-X. Chen, D. J. Young, T. S. A. Hor, *Angew. Chem. Int. Ed.* **2014**, 53, 4628–4632.; (b) C. R. Murdock, B. C. Hughes, Z. Lu, D. M. Jenkins, *Coord. Chem. Rev.* **2014**, 258, 119–136.
- [6] (a) H.-J. Kim, W.-C. Zin, M. Lee, *J. Am. Chem. Soc.* **2004**, 126, 7009–7014.; (b) C.R. M. O. Matos, F. G. A. Monteiro, F. D. S. Miranda, C. B. Pinheiro, A. D. Bond. C. M. Ronconi, *Cryst. Growth Des.* **2017**, 17, 5965–5974.; (c) E. Lee, K.-M. Park, M. Ikeda, S. Kuwahara, Y. Habata, S. S. Lee, *Inorg. Chem.* **2015**, 54, 5372–5383.; (d) E. Lee, H. Ju, S. Kim, K.-M. Park, S. S. Lee, *Cryst. Growth Des.* **2015**, 15, 5427–5436.
- [7] (a) A. Tarassoli, V. Nobakht, E. Baladi, L. Carlucci, D. M. Proserpio, *CrystEngComm*, **2017**, 19, 6116–6126.; (b) S. Azizzadeh, V. Nobakht, L. Carlucci, D. M. Proserpio, *Polyhedron*, **2017**, 130, 58–66.; (c) A. Beheshti, W. Clegg, V. Nobakht, R.W. Harrington, *Cryst. Growth Des.* **2013**, 13, 1023–1032; (d) A. Beheshti, V. Nobakht, S. K. Behbahanzadeh, C. T. Abrahams, G. Bruno, H. A. Rudbarid, *Inorg. Chim. Acta.* **2015**, 437, 20–25; (d) A. Beheshti, W. Clegg, V. Nobakht, R. W. Harrington, *Polyhedron*, **2014**, 81, 256–260.
- [8] J. F. Ma, J. F. Liu, Y. Xing, H. Q. Jia, Y. H. Lin, *J. Chem. Soc. Dalton Trans.* **2000**, 2403–2407.
- [9] Mercury 3.0, Copyright Cambridge Crystallographic Data Centre, 12 Union Road, Cambridge, CB2 1EZ, UK, **2012**.
- [10] G. M. Sheldrick, SHELX97-Programs for Crystal Structure Analysis, release 97-2; Institut für Anorganische Chemie der Universität Göttingen, Göttingen, Germany, **1998**.
- [11] A. Tabacaru, S. Galli, C. Pettinari, N. Masciocchi, T. M. McDonald, J. R. Long, *CrystEngComm*, **2015**, 17, 4992–5001.
- [12] (a) E. Arunan, G.R. Desiraju, R.A. Klein, J. Sadlej, S. Scheiner, I. Alkorta, D.C. Clary, R.H. Crabtree, J.J. Dannenberg, P. Hobza, H.G. Kjaergaard, A.C. Legon, B. Mennucci, D.J. Nesbitt, J.

- Pure. Appl. Chem. **2011**, 83, 1637-1641; (b) S. Brooker, N.G. White, A. Bauza, P.M. Deya, A. Frontera, Inorg. Chem., **2012**, 51, 10334-10340; (c) L. Carlucci, G. Ciani, S. Maggini, D.M. Proserpio, CrystEngComm, **2008**, 10, 1191-1203.
- [13] C. Janiak, J. Chem. Soc., Dalton Trans. **2000**, 3885-3896.
- [14] A. L. Spek, J. Appl. Crystallogr. **2003**, 36, 7-13.
- [15] (a) M. Xu, S.-S. Yang, Z.-Y. Gu, Chem. Eur. J. **2018**, 24, 15131–15142; (b) M. Liu, K. Xie, M. D. Nothling, P. A. Gurr, S. S. L. Tan, Q. Fu, P. A. Webley, G. G. Qiao, ACS Nano, **2018**, 12, 11591–11599.
- [16] K. V. Domasevitch, P. V. Solntsev, I. A. Gural'skiy, H. Krautscheid, E. B. Rusanov, A. N. Chernega, J. A. K. Howard, Dalton Trans. **2007**, 3893–3905.
- [17] V. Nobakht, A. Beheshti, D. M. Proserpio, L. Carlucci, C. T. Abrahams, Inorg. Chim. Acta. **2014**, 414, 217–225.
- [18] A. Lalegani, M. Khalaj, S. Sedaghat, K. Łyczko, J. Lipkowski, J. Mol. Struct. **2017**, 1148, 479-485.
- [19] (a) L. Carlucci, G. Ciani, D. M. Proserpio, A. Sironi, Inorg. Chem. **1998**, 37, 5941-5943. (b) Y.-F. Li, Z.-H. Pan, T.-J. Lou, Acta Cryst. **2007**, C63, m516-m518.
- [20] A. Bondi, J. Phys. Chem. **1964**, 68, 441–451.
- [21] K. Fukuhara, S.-i. Noro, K. Sugimoto, T. Akutagawa, K. Kubo, T. Nakamura, Inorg. Chem. **2013**, 52, 4229-4237.
- [22] Rosenthal, M. R. J. Chem. Educ. **1973**, 50, 331–334.
- [23] W. Huang, R. Frech, R. A. Wheeler, J. Phys. Chem. **1994**, 98, 100-110.

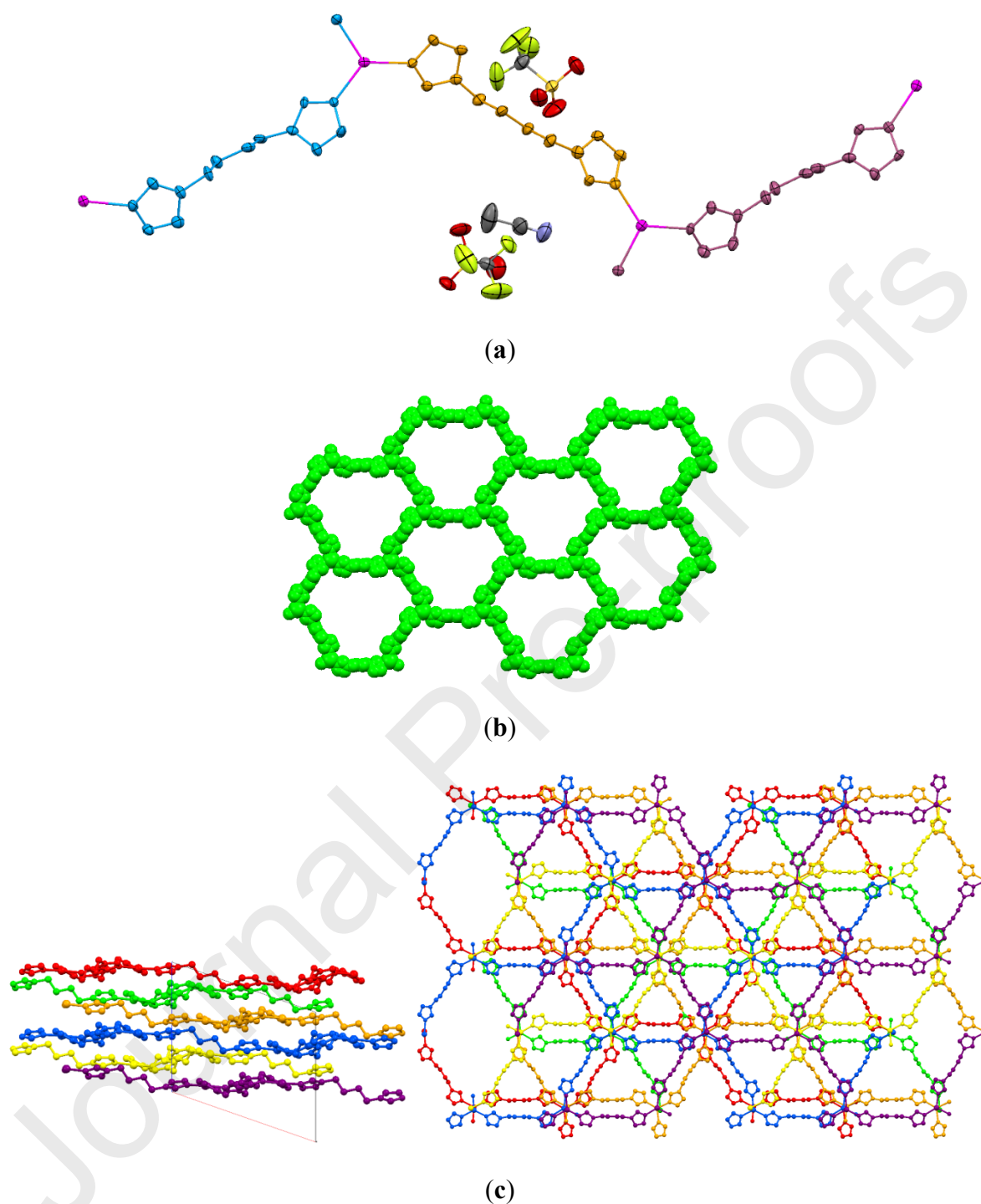


Figure 1. The structure of $\{[Ag_2(\mu\text{-bib})_3](SO_3CF_3)_2 \cdot (CH_3CN)}_n$ (**1**). (a) Asymmetric unit of **1** with additional atoms to complete the coordination environment of Ag. (b) 2D honeycomb structure with large hexagon windows. (c) Views along the $[0\ 1\ 0]$ (left) and $[0\ 0\ 1]$ (right) directions of the unusual ABCDEF packing mode of six parallel **hcb** sheets.

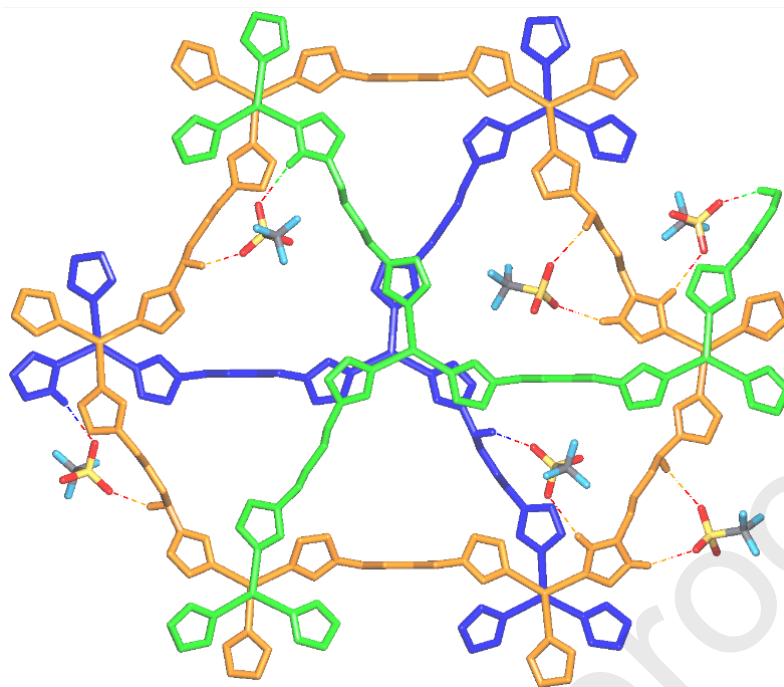


Figure 2. Non-classic C-H...O interactions of triflate ions with cationic network of **1**.

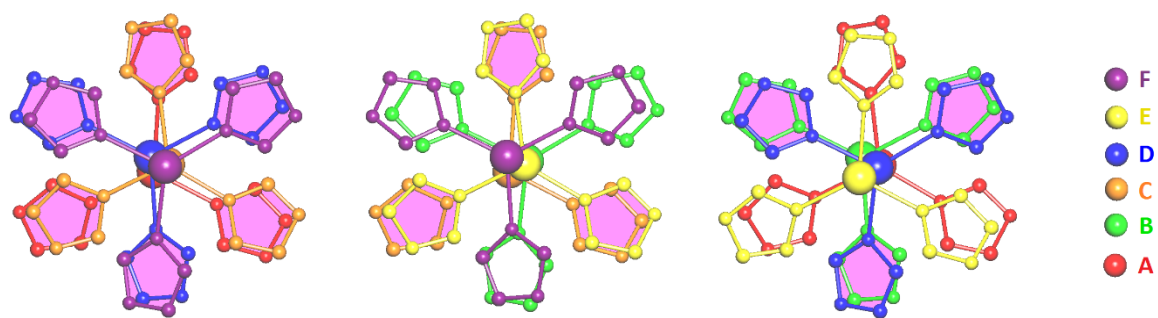


Figure 3. Representation of the $\pi \cdots \pi$ stacking interactions between imidazolyl rings of the layers A and C, B and D, C and E, and D and F in compound 1.

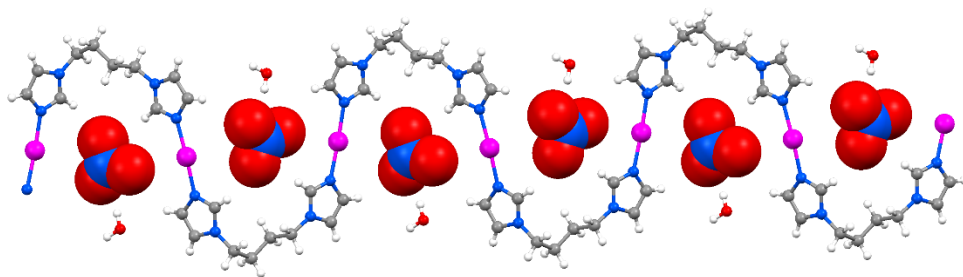


Figure 4. View of 1-D zig-zag chain structure of **2** along the *b* axis. Nitrate ions (spacefill representation) and water molecules are located on alternate sides of the chain.

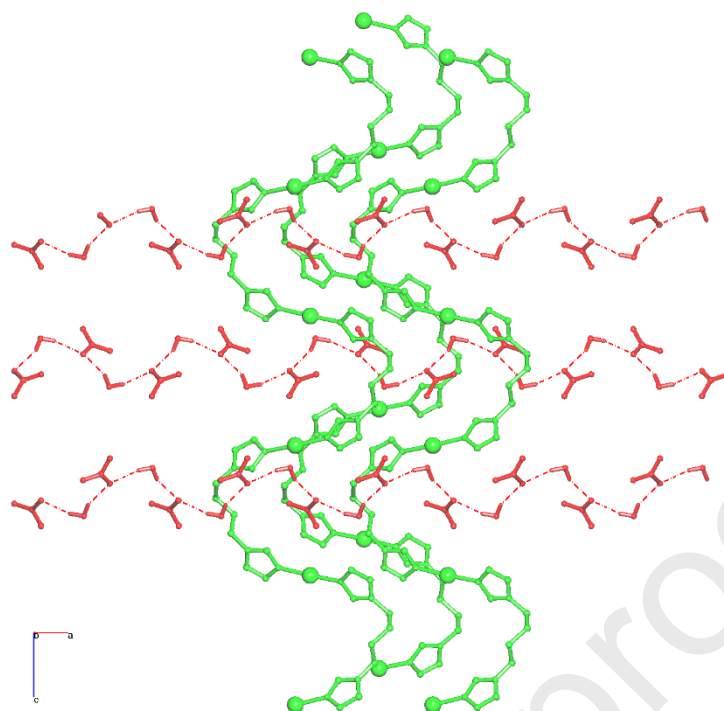


Figure 5. View along the *b* axis of two 1D chains of $[\text{Ag}(\mu\text{-bib})]_n^+$ (green) and of water – nitrate hydrogen bonded chains (red) showing their mutually perpendicular disposition in compound **2**.

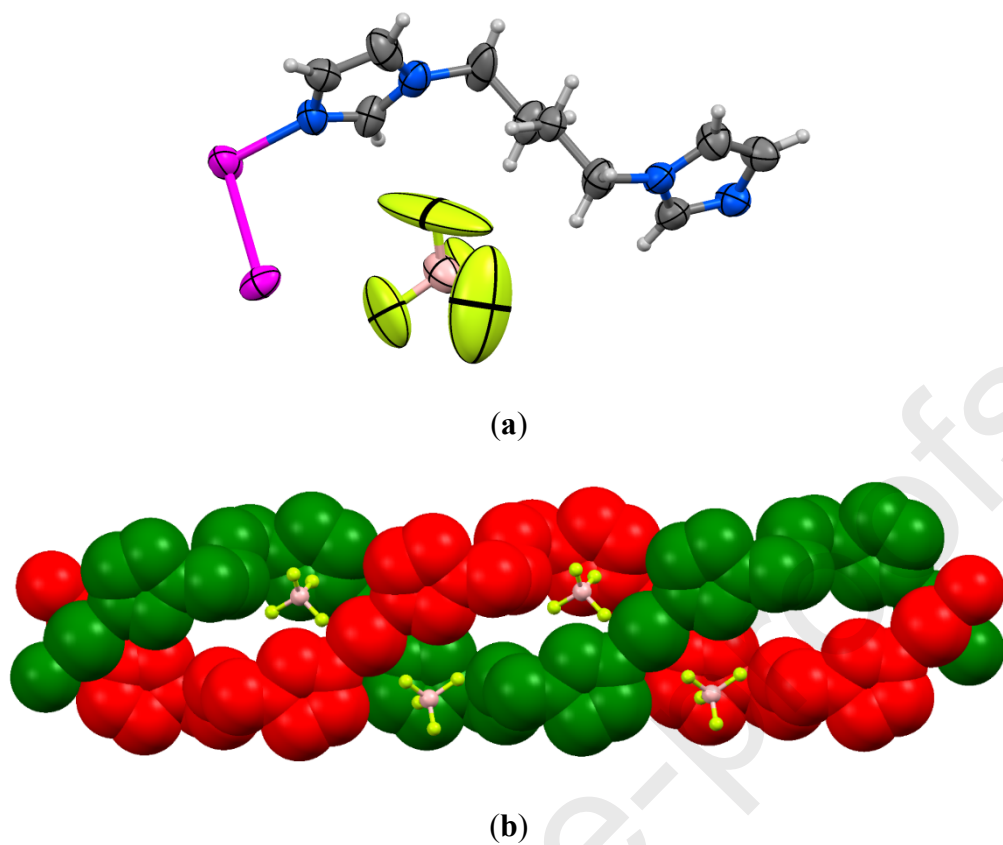


Figure 6. The structure of $\{[\text{Ag}(\mu\text{-bib})](\text{BF}_4)\}_n$ (**3**). a) Asymmetric unit and b) the double helix.

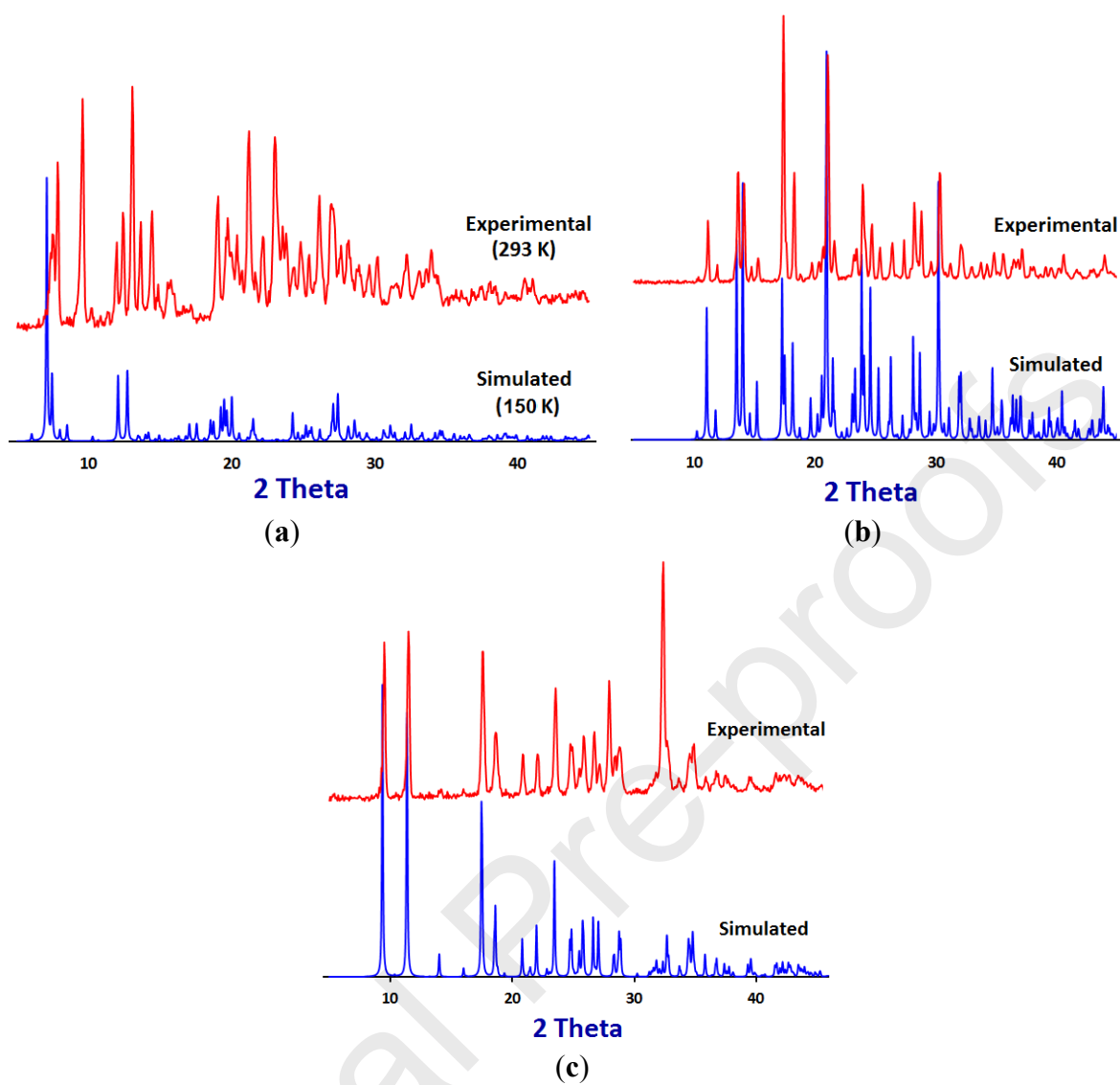


Figure 7. Observed (red) and calculated (blue) powder X-ray diffraction patterns for compounds: a) 1, b) 2 and c) 3.

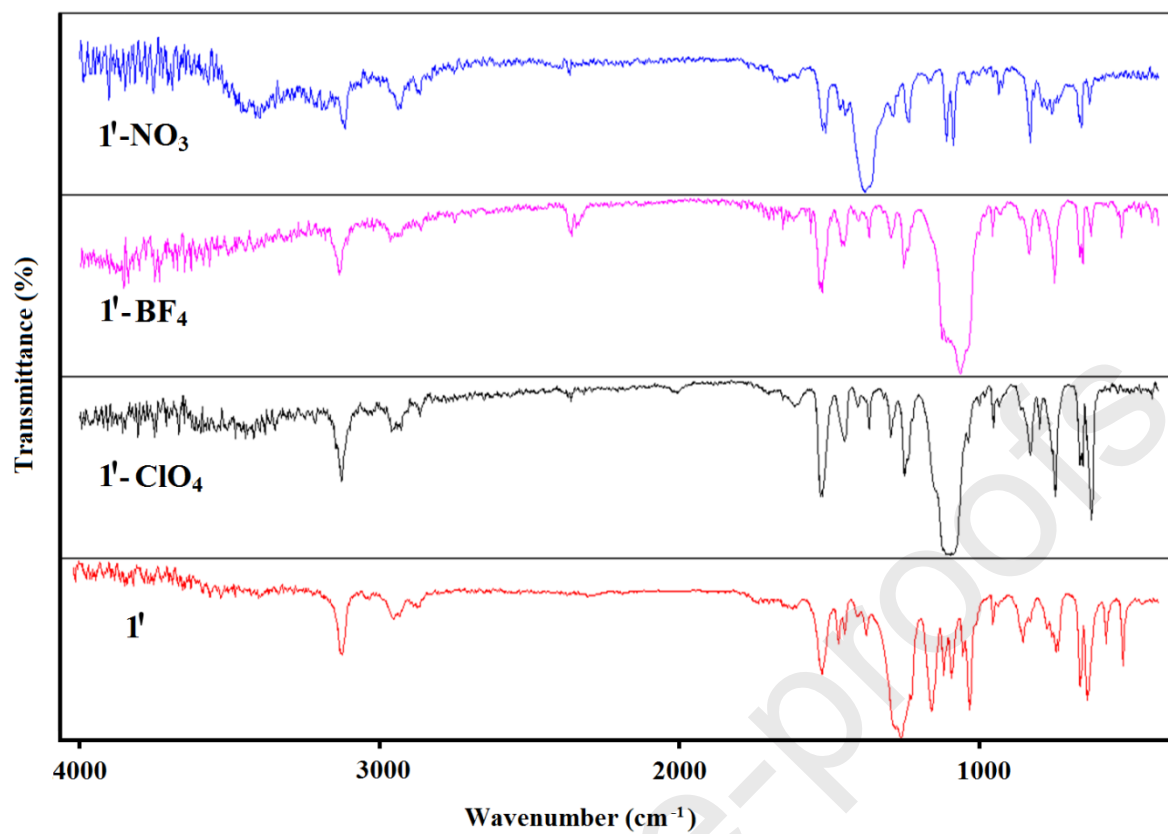


Figure 8. FT-IR spectra for **1'** and anion exchanged products **1'-ClO₄**, **1'-BF₄**, and **1'-NO₃**.

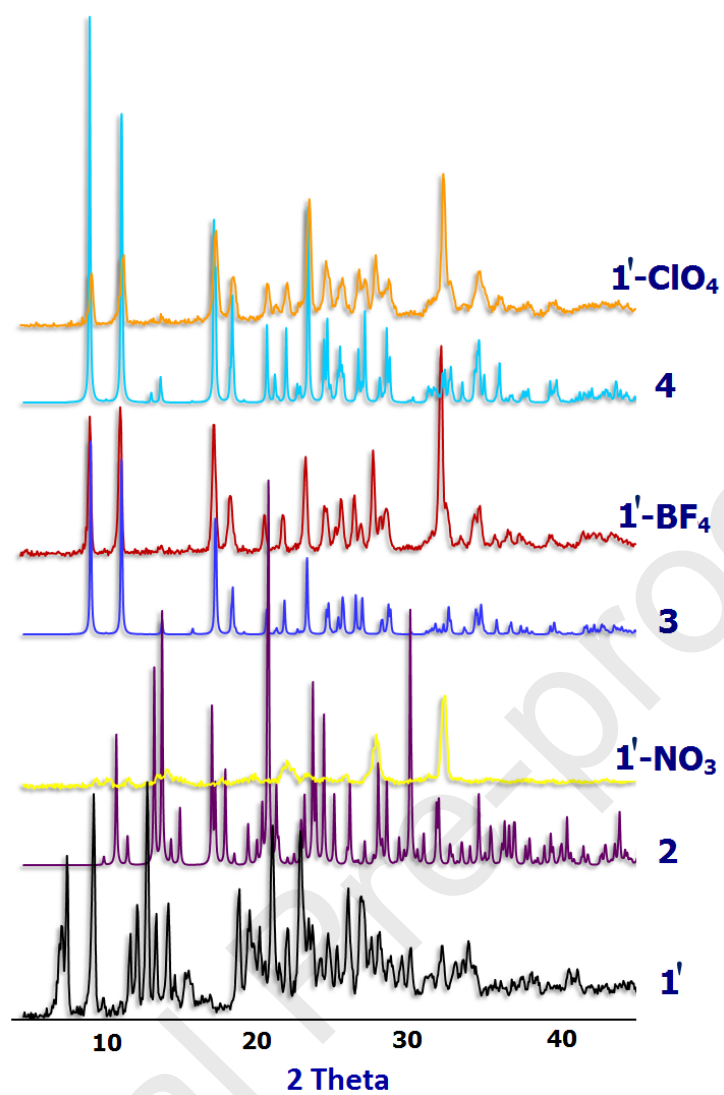


Figure 9. PXRD patterns for 1'-4 and anion exchanged products 1'-NO₃, 1'-BF₄, and 1'-ClO₄.

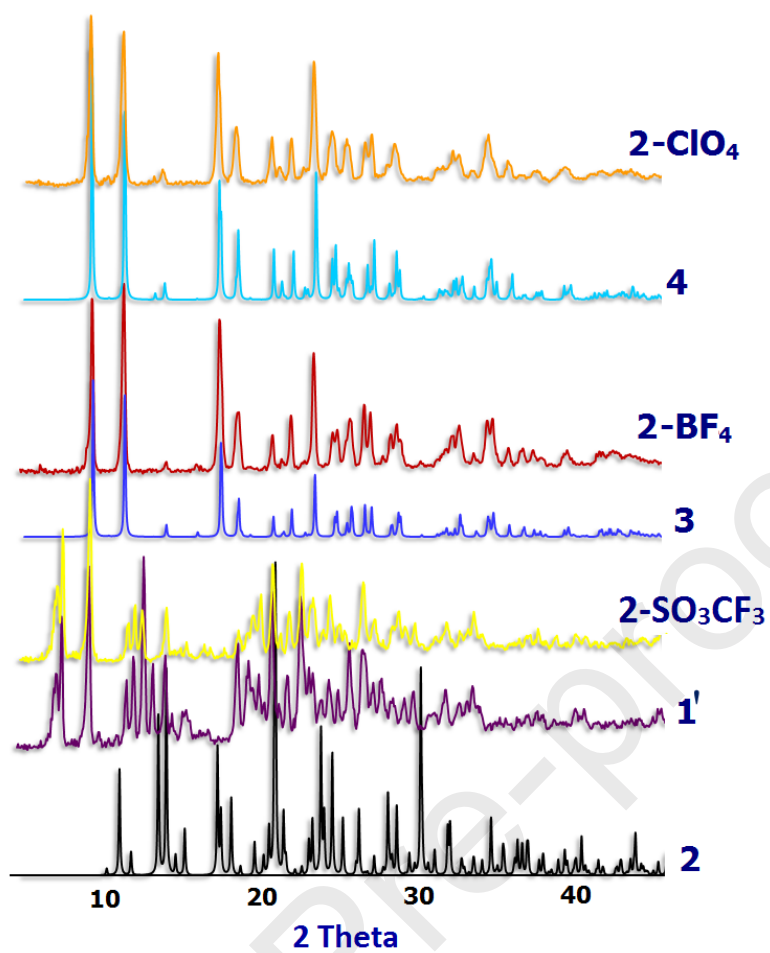


Figure 10. PXRD patterns for 1'-4 and anion exchanged products 2-SO₃CF₃, 2-BF₄, and 2-ClO₄.

Table 1. Crystallographic data and structure refinement details for **1–3**

Compound	1	2	3
Formula	C ₃₀ H ₄₂ Ag ₂ N ₁₂ ,2(CF ₃ O ₃ S),C ₂ H ₃ N	C ₁₀ H ₁₆ AgN ₄ O,NO ₃	C ₁₀ H ₁₄ AgN ₄ ,BF ₄
Formula mass	1125.69	378.15	384.93
<i>T</i> (K)	150	293	293
Cryst. Syst.	Monoclinic	Orthorhombic	Monoclinic
Space group	<i>P</i> 21/ <i>c</i>	<i>P</i> 2 ₁ 2 ₁ 2 ₁	<i>C</i> 2/ <i>c</i>
<i>a</i> (Å)	15.525(3)	8.5056(4)	11.0558(6)
<i>b</i> (Å)	23.716(4)	10.2635(4)	13.3716(7)
<i>c</i> (Å)	13.222(2)	16.0148(7)	18.8428(10)
α (°)	90	90	90
β (°)	109.189(3)	90	90.750(1)
γ (°)	90	90	90
<i>V</i> (Å ³)	4597(14)	1398.05(11)	2785.4(3)
<i>Z</i>	4	4	8
<i>D</i> calcd (g cm ⁻³)	1.622	1.797	1.836
Data collected	51736	27724	32676
Unique data (<i>R</i> _{int})	10371	4528 (0.016)	4545 (0.018)
Data/restraints/params	10371/0/569	4528/0/190	4545/0/182
<i>R</i> 1[<i>I</i> > 2σ(<i>I</i>)]	0.133	0.0215	0.0448
w <i>R</i> ₂ (all data)	0.3220	0.0586	0.1474

Table 2. Hydrogen bonds in compounds 1-3.

Three cationic	D-H...A	D-H/Å	H...A/Å	D-A/Å	D-H...A/°	new Ag(I)-
	(1)					
	C9-H9...O6 ^a	0.9300	2.4900	3.35(3)	153.00	
	C51-H51B...O4 ^b	0.9700	2.5600	3.51(2)	167.00	
	C40-H40...O2 ^b	0.9300	2.5100	3.39(2)	158.00	
	C81-H81A...O4	0.9700	2.5800	3.32(2)	132.00	
	C83-H83B...O3 ^c	0.9700	2.5600	3.47(3)	156.00	
	C8-H8...N123 ^d	0.9300	2.6100	3.52(3)	168.00	
Symmetry operations: <i>a</i> - <i>l</i> + <i>x</i> , <i>y</i> ,- <i>l</i> + <i>z</i> ; <i>b</i> <i>x</i> , <i>l</i> /2- <i>y</i> ,- <i>l</i> /2+ <i>z</i> ; <i>c</i> <i>l</i> - <i>x</i> , <i>l</i> - <i>y</i> , <i>l</i> - <i>z</i> ; <i>d</i> - <i>l</i> + <i>x</i> , <i>y</i> ,- <i>l</i> + <i>z</i>						
(2)						
	O20-H1W...O10 ^a	0.85(4)	2.03(4)	2.860(4)	164(4)	
	O20-H2W...O10 ^b	0.87(4)	2.00(4)	2.822(4)	157(4)	
	O20-H2W...O12 ^b	0.87(4)	2.57(4)	3.323(5)	146(4)	
	C20-H20...O12	0.9300	2.5500	3.364(4)	146.00	
	C60-H60A...O20 ^c	0.9700	2.5900	3.521(4)	161.00	
Symmetry operation: <i>a</i> - <i>x</i> , <i>l</i> /2+ <i>y</i> , <i>3</i> /2- <i>z</i> ; <i>b</i> <i>l</i> /2- <i>x</i> , <i>l</i> - <i>y</i> , <i>l</i> /2+ <i>z</i> ; <i>c</i> <i>l</i> - <i>x</i> ,- <i>l</i> /2+ <i>y</i> , <i>3</i> /2- <i>z</i>						
(3)						
	C2-H2...F1 ^a	0.9300	2.4700	3.272(7)	145.00	
	C3-H3...F3	0.9300	2.4900	3.202(7)	134.00	
	C4-H4B...F3 ^b	0.9700	2.3500	3.012(6)	125.00	
	C7-H7B...F4 ^c	0.9700	2.3700	3.197(5)	143.00	
	C8-H8...F4 ^c	0.9300	2.2800	3.193(4)	166.00	
Symmetry operation: <i>a</i> <i>x</i> , <i>l</i> - <i>y</i> , <i>l</i> /2+ <i>z</i> ; <i>b</i> 2- <i>x</i> , <i>y</i> , <i>3</i> /2- <i>z</i> ; <i>c</i> 3/2- <i>x</i> ,- <i>l</i> /2+ <i>y</i> , <i>3</i> /2- <i>z</i>						

coordination polymers of a flexible ligand and weakly coordinating anions, SO₃CF₃⁻, BF₄⁻, and NO₃⁻, have been successfully isolated and characterized. The compounds show different structures and dimensionalities. Anion exchange experiments reveal interesting structural changes in solution of different anions.

